

RESEARCH ARTICLE | MAY 23 2016

Ultra-precision fabrication of 500 mm long and laterally graded Ru/C multilayer mirrors for X-ray light sources

M. Störmer; H. Gabrisch; C. Horstmann; U. Heidorn; F. Hertlein ; J. Wiesmann; F. Siewert; A. Rack



Rev. Sci. Instrum. 87, 051804 (2016)

<https://doi.org/10.1063/1.4950748>



View
Online



Export
Citation

CrossMark

Articles You May Be Interested In

The New Materials Science Beamline HARWI-II at DESY

AIP Conference Proceedings (January 2007)

Simulation framework SYRIS tested for microtomography applications at the imaging beamline P05/PETRA III

AIP Conference Proceedings (January 2019)

HARWI-II, The New High-Energy Beamline for Materials Science at HASYLAB/DESY

AIP Conference Proceedings (May 2004)

500 kHz or 8.5 GHz?
And all the ranges in between.

Lock-in Amplifiers for your periodic signal measurements



Find out more

 Zurich
Instruments

Ultra-precision fabrication of 500 mm long and laterally graded Ru/C multilayer mirrors for X-ray light sources

M. Störmer,^{1,a)} H. Gabrisch,¹ C. Horstmann,¹ U. Heidorn,² F. Hertlein,² J. Wiesmann,² F. Siewert,³ and A. Rack⁴

¹*Helmholtz-Zentrum Geesthacht, Institute of Materials Research, Max-Planck-Straße 1, D-21502 Geesthacht, Germany*

²*Incoatec GmbH, Max-Planck-Str. 2, D-21502 Geesthacht, Germany*

³*Helmholtz-Zentrum Berlin, Albert-Einstein-Straße 15, D-12489 Berlin, Germany*

⁴*European Synchrotron Radiation Facility, CS 40220, 38043 Grenoble, France*

(Received 22 December 2015; accepted 4 April 2016; published online 23 May 2016)

X-ray mirrors are needed for beam shaping and monochromatization at advanced research light sources, for instance, free-electron lasers and synchrotron sources. Such mirrors consist of a substrate and a coating. The shape accuracy of the substrate and the layer precision of the coating are the crucial parameters that determine the beam properties required for various applications. In principal, the selection of the layer materials determines the mirror reflectivity. A single layer mirror offers high reflectivity in the range of total external reflection, whereas the reflectivity is reduced considerably above the critical angle. A periodic multilayer can enhance the reflectivity at higher angles due to Bragg reflection. Here, the selection of a suitable combination of layer materials is essential to achieve a high flux at distinct photon energies, which is often required for applications such as microtomography, diffraction, or protein crystallography. This contribution presents the current development of a Ru/C multilayer mirror prepared by magnetron sputtering with a sputtering facility that was designed in-house at the Helmholtz-Zentrum Geesthacht. The deposition conditions were optimized in order to achieve ultra-high precision and high flux in future mirrors. Input for the improved deposition parameters came from investigations by transmission electron microscopy. The X-ray optical properties were investigated by means of X-ray reflectometry using Cu- and Mo-radiation. The change of the multilayer d-spacing over the mirror dimensions and the variation of the Bragg angles were determined. The results demonstrate the ability to precisely control the variation in thickness over the whole mirror length of 500 mm thus achieving picometer-precision in the meter-range. © 2016 Author(s). All article content, except where otherwise noted, is licensed under a Creative Commons Attribution (CC BY) license (<http://creativecommons.org/licenses/by/4.0/>). [<http://dx.doi.org/10.1063/1.4950748>]

11 October 2023 12:38:15

I. INTRODUCTION

Multilayer mirrors are now widely used in a variety of laboratory instruments such as X-ray diffractometers and X-ray fluorescence spectrometers, and increasingly at synchrotron storage rings. The typical length of these mirrors of about 100 mm was determined by manufacturing capabilities. Today a substrate length of about 1000 mm is available and coating technology has been developed for longer mirrors. At Helmholtz-Zentrum Geesthacht (HZG), we have installed a magnetron sputtering facility for a mirror length of 1500 mm.

The advantage of a multilayer is that it offers a stronger beam deflection than a single layer, which only reflects below the critical angle due to total external reflection. At grazing and normal incidence, a multilayer provides a higher reflectivity of X-rays due to Bragg reflection.^{1,2} In the range of high photon energies, the dispersion ($\delta < 10^{-4}$) is important and the absorption ($\beta < 10^{-6}$) can be neglected.³

Then, the corrected Bragg condition is

$$m\lambda = 2d \sin \theta_{B,m} \sqrt{1 - \frac{2\bar{\delta}}{\sin^2 \theta_{B,m}}}, \quad (1)$$

where λ is the wavelength, m is an integer, d is the period, $\theta_{B,m}$ is the measured Bragg angle, and

$$\bar{\delta} = \frac{1}{d} \sum_{i=1}^N d_i \cdot \delta_i \quad (2)$$

is the bi-layer weighted real part of the refractive index. The specifications of a multilayer depend on the particular application. They include the required X-ray wavelength or photon energy,⁴ the selection of the materials,⁵ and their inner structure. The geometrical shape of the substrate is also important, since the slope error of a mirror or a grating may cause unwanted wavefront distortions that impair the imaging properties of a mirror.⁶⁻⁸ Furthermore the aberrations in curved multilayers have a large effect on the imaging properties.^{9,10}

Depending on the inner structure of the stack of materials, two main types of multilayers can be distinguished. First,

^{a)}michael.stoermer@hzg.de.



multilayers with a constant period d are used as analyzer or filter in an X-ray fluorescence spectrometer to detect a distinct chemical element in a complex sample. Thus, it is possible to quantify the elemental concentration, e.g., in a boron-analyzer.¹¹ Second, laterally graded multilayers are applied as beam shaper and monochromator in X-ray diffractometers. A laterally graded multilayer mirror combines the advantages of a totally reflecting mirror (i.e., high integral reflectivity) and of a crystal (i.e., monochromatization).^{12–14} Currently three types of laterally graded multilayer mirrors are used in X-ray diffractometry, namely, parabolic, elliptical, and planar, which generate a parallel, focused, or divergent beam, respectively. The thickness profiles of these multilayers have to fulfill the Bragg condition at each position in the entire optical area. In fact, a small variation in the multilayer period along the mirror length is required. The difference in period over a mirror length of 100 mm is 1 nm; therefore, the required mean gradient is about $1 \text{ nm}/100 \text{ mm} = 10^{-8}$.

The challenges of multilayer fabrication are to deposit a suitable combination of layer materials and to precisely tune the thickness along the mirror length and perpendicular to it. Some thin-film techniques offer this, for instance, magnetron sputtering, thermal evaporation, and pulsed laser deposition.² When using magnetron sputtering it is crucial to understand the relevant parameters that determine the resulting thickness distribution.^{15–18} Present thin-film techniques are able to manufacture films of excellent thickness uniformity¹⁹ and furthermore, to tailor a desired thickness gradient in the tangential and sagittal directions. For extreme ultraviolet (EUV) optics, a very small variation in period of the Mo/Si multilayers is required.^{20–23} Here, the coating specifications for thickness uniformity and gradient are very tight, requiring a tolerance band better than $\pm 0.1\%$ of the overall coating period. The reflectance of these Mo/Si coatings is typically above 65% and the local deviation in the multilayer period is controlled to smaller than 15 pm over a typical diameter of the optical elements of 140 mm.

Multilayers are becoming more widely used as optical elements in beamlines at current synchrotron sources since they can align, guide, and monochromatize an X-ray beam for imaging, focusing, and parallelizing applications.²⁴ For one of the beamlines at PETRA III the use of a double-multilayer monochromator (DMM) is now proposed to provide a high photon flux and an offset.²⁵ The effect of the multilayer period and the number of layers on the optical performance were investigated on a selection of materials in various multilayers.^{6,26,27} The results showed that the material composition is a dominant factor in mirror performance. Multilayer optics in synchrotron beamlines can be used to shape the X-ray beam;^{28,29} thus, on using the Kirkpatrick-Baez configuration (KB optics)³⁰ a high photon flux can be directed onto small samples. This configuration is also often installed for vertical focusing and horizontal focusing of the X-ray beam and consists of two crossed, elliptically curved mirrors.³¹ In this case, curved graded multilayers are employed as nanofocusing elements for the X-ray beam. The meridional multilayer d -spacing gradient plays a crucial role, since it guarantees uniform reflectivity and phase, thus ensuring clean focal spots and high photon flux.

The selection of ruthenium/carbon (Ru/C) is a suitable material combination for the intermediate photon energy of about 15 keV, which is interesting for synchrotron applications, in particular, for tomographic imaging³² and studies of molecular reaction dynamics.³³ Low-temperature properties of Ru/C multilayers were investigated before and after cryogenic cooling.³⁴ Earlier studies of Ru-containing multilayers showed that the crystallinity affects the multilayer quality, particularly the roughness and diffusion at the interface. The perfection of the multiple stack can be improved by the presence of an amorphous layer; therefore, the selected sputtering conditions of the materials are important to accomplish the best possible reflectivity.^{35–37} This has been demonstrated at some synchrotron sources, where multilayers of Ru/B₄C are used in monochromators for this mid-energy range.^{24,28} In these cases, a spacer of B₄C was selected that acts as an excellent barrier against compound formation at the interfaces. Regarding mirror dimensions, nowadays, synchrotron and free-electron laser (FEL) beamlines require multilayer mirrors with a length of at least 500 mm and perhaps more in the near future.

In this contribution, the development of a very long, high-flux Ru/C multilayer mirror with an ultra-precise thickness variation and a small bandwidth is reported. The challenge is to achieve an elliptical variation in the multilayer period of better than $\pm 0.3\%$ with a maximum difference in period of 75 pm over a mirror length of 500 mm resulting in an extremely small mean gradient of about 10^{-10} .

It is important to mention that the sputtering facility of the Helmholtz-Zentrum Geesthacht (HZG) is designed to develop and optimise the preparation of mirrors having a length of 1500 mm with ultra-high precision in thickness uniformity over the entire deposition area. These can be single layer mirrors for total-reflection or high-flux multilayer mirrors.^{38,39} Current and upcoming advanced light sources need very long mirrors to distribute the peak power over a large footprint to avoid radiation damage to the mirror.^{40–43} The question arises whether it is possible to increase the mirror length while maintaining the high precision in controlling the layer thickness that is feasible today in the case of smaller substrates, as mentioned above. The overall aim is the reproducible preparation of a 500 mm long Ru/C multilayer mirror with an elliptically shaped variation of the multilayer period within a very small error margin. The specified mean gradient of about 10^{-10} in the tangential direction is extremely small. For a mirror length of 500 mm it translates into a maximum permitted change in period of only 75 pm or to continuously changing the ideal incidence angle from 28 mrad to 29.7 mrad in the tangential direction. Variations in thickness and theta perpendicular to the tangential direction were also studied since a constant multilayer period over some tens of millimeters is required in the sagittal direction of the mirror. The final optical system requires two identical multilayer mirrors to provide a high flux and a tuneable energy resolution.

II. EXPERIMENTAL

The Ru/C multilayer films were deposited in the HZG magnetron sputtering facility measuring 4.5 m in length, which is equipped with a load lock, and which is evacuated by a turbo

molecular pump and a cryo pump.^{44,45} The base pressure of the system is typically below 10^{-5} Pa. A laminar flow box of 2 m height is used for the pre-treatment and for the cleaning of the uncoated substrates. Small silicon substrates having a typical surface roughness of 0.3 nm rms were used for calibration. A vacuum interlock system provides a quick sample exchange. The deposition chamber has two fixed rectangular magnetron-sputtering sources (355 mm \times 88.9 mm) covered with high purity materials. Further typical parameters are a distance of 14 cm between source and substrate and an argon gas pressure of 0.12 Pa. The purity of the argon is 99.999 99%. The sputtering conditions for carbon deposition were optimized at a power of 1000 W, a frequency of 40 kHz, a reverse time of 1 μ s and for ruthenium deposition to a power of 120 W DC. Some calibration runs with 30 pairs of Ru/C are performed before multilayers with 100, 150, and 200 pairs are manufactured requiring deposition times of 4, 8.5 and 10 h, respectively. Several small silicon substrates measuring 20 mm by 60 mm were placed onto the movable carrier that served to determine the variation in thickness along the tangential (*x*-) and the sagittal (*y*-) directions. Seven small substrates were placed in the tangential direction in the center of the carrier (*y* = -60 mm) and two substrates were placed in the perpendicular direction at four *x*-positions 10, 150, 350, and 490 mm. Several final calibration runs were performed with two Si substrates in order to investigate the tangential thickness gradient precisely without the influence of short substrates. The substrates measure about 250 mm in length and 700 μ m in thickness and have a very low surface roughness of less than 0.2 nm rms. The final two planar Si blanks have a micro-roughness of 0.1 nm rms and are of the dimensions 400 mm \times 30 mm \times 19 mm with an optical area of 386 mm \times 20 mm. The carrier velocity ranged from 5 mm/s to 30 mm/s whereby a higher carrier velocity results in a lower layer thickness. The combination of generator power, argon gas pressure, and the carrier velocity determines the layer thickness in the multilayer stack. The calibration of the carrier movement for C deposition was performed in two steps. First W/C was deposited instead of Ru/C in order to determine the velocity and acceleration of the carrier for carbon deposition with a very small gradient in thickness according to the elliptically shaped variation in multilayer period. The second part of the calibration was focused mainly on Ru using the optimised values for the deposition of C. All parameters are precisely controlled and monitored since the carrier movement needs to be very stable and reproducible throughout the whole deposition process of 200 pairs. The use of a tunable acceleration drive is also important in order to vary the thickness along the mirror length precisely and to achieve the desired gradient.

The X-ray optical properties of the magnetron-sputtered Ru/C-multilayers were investigated by means of X-ray reflectometry (XRR) with laboratory sources (Cu: 8048 eV and Mo: 17 480 eV). Typically, the incidence beam of a diffractometer (D8 Advance, Bruker) is 1 mm high and 20 mm wide using a line focus tube. The local changes of these properties were analyzed as a function of the mirror dimensions, that is, in the tangential and sagittal directions. The step width of the reflectivity scans was 0.003° . The largest area measured was 500 mm \times 120 mm (i.e., 46 mirror positions). The measured

scans were analyzed to determine the Bragg angle and the multilayer period. The experimental results were compared with simulated x-ray reflectivity curves that were obtained using various software packages, e.g., IMD⁴⁶ and LEPTOS R.⁴⁷ Thus, period, reflectivity, roughness, and density of the multilayers were determined. Furthermore, the full width at half-maximum of the first order Bragg peak was estimated. Additionally, in some samples, the reflectivity was characterized using Mo radiation at 17.48 keV. This means that the X-ray optical properties of the multilayers were investigated below and above the specified photon energy range of about 15 keV.

For characterization by transmission electron microscopy (TEM), cross sections were prepared from the Ru/C multilayers by dimpling and ion milling. TEM investigations were performed in a Titan 80-300 kV TEM equipped with a Cs corrector and operated at 300 kV. The micro-roughness of the Ru/C multilayers on calibration samples was investigated by atomic force microscopy (AFM), which is a scanning probe microscopy (SPM) technique with a height resolution on the atomic scale.^{48,49} A Bruker SIS-Ultra-objective with a 40 μ m \times 40 μ m scanner at the AFM was used on a PICO-station system with active vibration damping. The tip used for these measurements in the non-contact mode was a silicon SPM-sensor with a resonance frequency of 190 kHz and a force constant of 48 N/m. The tip has a height of 10-15 μ m and a radius of less than 8 nm. Thus, the achievable lateral resolution is about 10 nm in a conservative estimate. After 10 scans the tip is changed to avoid measurements being influenced by tip wear.

III. RESULTS AND DISCUSSION

The combination of Ru/C multilayers has been selected because simulations by IMD showed that this combination provides a high X-ray reflectivity and a small width of the Bragg peak at intermediate photon energies of 15 keV. Therefore it is expected that an X-ray optical system of two Ru/C multilayer mirrors will achieve a high flux and a good energy resolution in a synchrotron beam, which is required for the investigation of very small crystals, especially proteins.

A. Optimization of the sputtering process after characterization by transmission electron microscopy (TEM)

The deposited multilayers were characterized by high-resolution imaging to identify the optimum deposition conditions that result in the best achievable optical properties of the Ru/C multilayers. The binary Ru-C phase diagram is nearly immiscible suggesting that there exists a driving force for a decomposition reaction.⁵⁰ Therefore, smooth and sharp interfaces between adjacent ruthenium and carbon layers are expected. The comparison between the microstructures resulting from two deposition conditions (Fig. 1(a), initial attempt) and (Fig. 1(b), optimized attempt) illustrates the effect the deposition condition has on the layer growth and on the final structure of the thin film. In Fig. 1(a) the Ru/C interfaces are wavy and the film structure consists of slightly misoriented, 20-60 nm wide columns. Such a columnar structure resulted

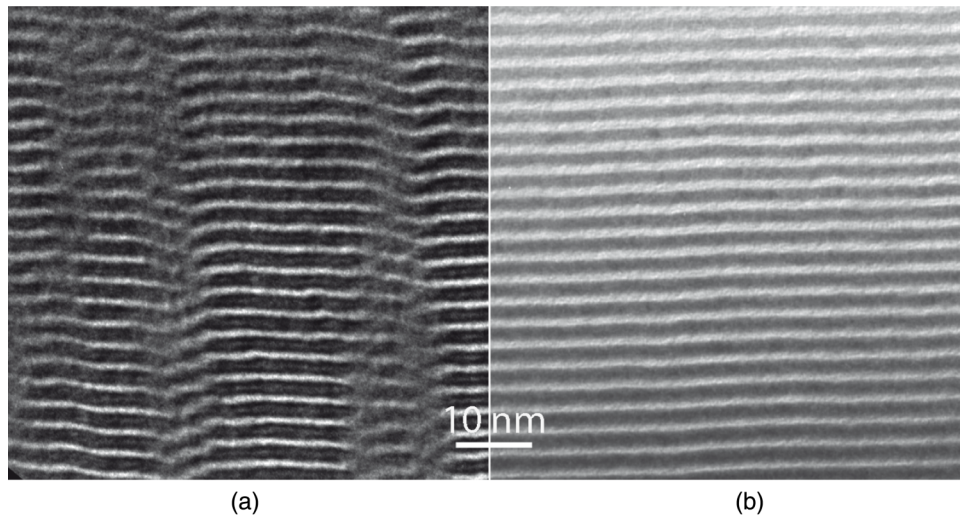


FIG. 1. High-resolution cross section TEM images of two Ru/C multilayers with a period of 2.76 nm and a thickness ratio of 0.49 prepared under different sputtering conditions: (a) wavy interfaces and 20–60 nm wide columns and (b) smooth and sharp interfaces with continuous and uniform layers.

in a low Cu X-ray reflectivity of about 40%. The optimized layer stack (Fig. 1(b)) exhibits an improved film quality with flat interfaces between amorphous carbon and nanocrystalline ruthenium layers. The sputtering conditions were: Ar gas pressure of 0.2 Pa: power of 400 W, mid frequency of 20 kHz, reverse time of 2 μ s for C and DC power of 80 W for Ru (initial) and Ar gas pressure of 0.1 Pa: power of 1000 W, mid frequency of 40 kHz, reverse time of 1 μ s for C and DC power 120 W for Ru (optimized). It is important to mention that silicon wafer substrates were used with a roughness of better than 0.3 nm rms according to the manufacturer's specifications. The improved layer structure results in an increase of the Cu reflectivity to 60%. Consequently, it is important to choose the right conditions for multilayer growth. In this case a higher generator power and longer free mean path length (due to lower argon gas pressure) in the vacuum chamber resulted in a higher X-ray reflectivity due to low interface roughness and suppressed interlayer diffusion.

B. Characterization of multilayers by X-ray reflectometry (XRR)

The reflectivity of a 500 mm long Ru/C multilayer was measured at various x-positions in the tangential direction of the mirror and the results are shown in Fig. 2. In the reflection curves, three orders of Bragg peaks were used to determine the X-ray optical properties, namely, period, roughness, and density. Additionally, the specular reflectivity of the first Bragg peak and the thickness ratio were determined at several mirror positions. The latter is given by $d_{\text{Ru}}/(d_{\text{Ru}} + d_{\text{C}})$. The mean reflectivity amounts to $60\% \pm 4\%$ and the thickness ratio is 0.420 ± 0.007 . Due to the reduction in thickness of the carbon layers along the mirror length, the reflectivity of the mirror is also slightly reduced due to stronger absorption in ruthenium layers. In Fig. 2, a gentle shift of the first Bragg peaks towards smaller angles is seen that results from the repeated slight change in velocity during fabrication of the layers. The precision of the coating process was very stable and reproducible during the preparation of the 200 Ru/C pairs. The

achieved period of the layer structure is continuously reduced as a function of the mirror length. The width of the Bragg peak is a further important factor for multilayer performance in an X-ray beamline since it defines the energy resolution. The mean full width at half maximum (FWHM) of the Bragg peak is about 1.1 mrad. In synchrotron applications, the width of the Bragg peak can be further reduced by a small angular change of the parallel alignment of the two multilayers with respect to each other—similar to the use of crystals in a double-crystal monochromator (DCM), e.g., Ref. 51. In Fig. 2 no broadening of the Bragg peak is detected. Small additional peaks were measured at 1.44° and 2.84° that are caused by the Cu- K_β radiation of the X-ray source. These small peaks further indicate a perfect multilayer structure. Therefore it is concluded that both layer materials, Ru and C, are separated by sub-atomic sharp interfaces, and that their periodicity is excellent over the whole stack of 200 pairs.

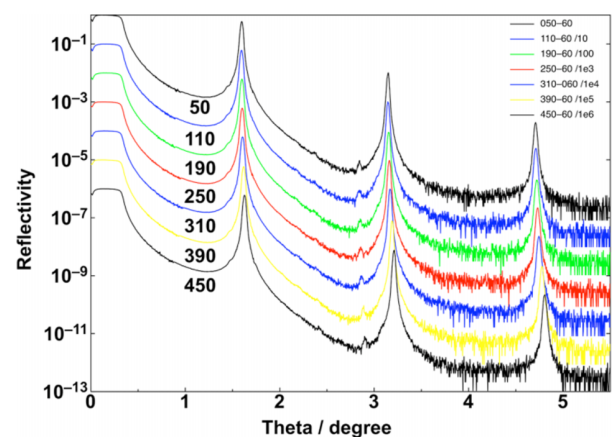


FIG. 2. Reflectometry measurements of a Ru/C multilayer recorded over an incidence angle of 5.5° with a step width of 0.003° using Cu radiation. The different curves were recorded at 7 positions over the deposition length of 500 mm. Due to a multilayer period of 2.82 nm and a thickness ratio of 0.42 three orders of Bragg peaks are clearly visible. The multilayer is deposited with a progressive increase in velocity in the tangential direction of the mirror that leads to a slight increase in the theta angle of the first-order peak from 1.597° to 1.627° .

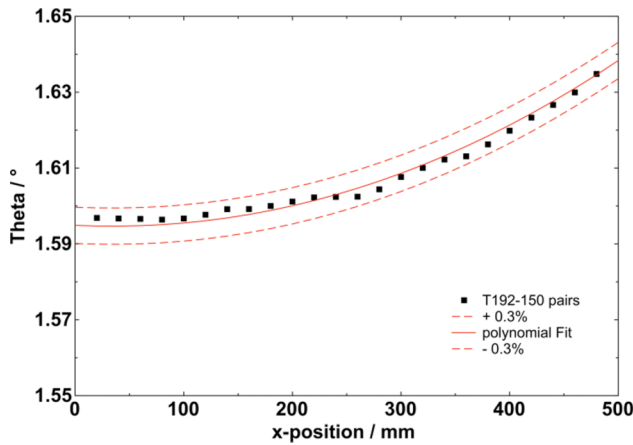


FIG. 3. Measured incidence angle as a function of the x-position (along the tangential direction) of a multilayer mirror with 150 Ru/C pairs at 24 x-positions (squares) using Cu radiation. The solid line represents a fit to the data and the dashed line shows the specified error band of $\pm 0.3\%$. In the center the incidence angle is 1.602° or 28.0 mrad; therefore, the multilayer period is 2.815 nm. The incidence angle starts at 1.597° (left edge), increases progressively, and ends at 1.635° over 480 mm.

C. Elliptically graded Ru/C multilayers with a period error of less than $\pm 0.2\%$ over a mirror length of 500 mm

The variation of the incidence angle along the tangential direction of a multilayer mirror with 150 Ru/C pairs is shown in Fig. 3. The incidence angle increases slightly with increasing x-position. The non-linear variation starts at 1.597° and ends at 1.635° measured over a length of 480 mm. The error of each determination of the incidence angle is less than 0.001° or $20 \mu\text{rad}$, in a conservative estimate. In the center of the mirror the incidence angle (i.e. theta) is 1.602° or 28.0 mrad, corresponding to a period of 2.815 nm. The measured thickness varied from 2.825 nm at the left edge to 2.758 nm at the right edge. Such an elliptical shape is required for focusing applications in a synchrotron beamline. The solid line in Fig. 3 represents the fitted curve. The nominal error band (dashed lines) is quite narrow with a tolerance of $\pm 0.3\%$. The desired elliptical shape in the tangential direction was achieved within the specified error band of $\pm 0.3\%$. The deviation was almost constant from run-to-run. An estimate of the best experimental deviation margin amounts to $\pm 0.17\%$. This result was reproduced several times while varying the number of periods, as described below. It can be concluded that this multilayer fabrication process is stable and reproducible in the range of the required picometer-precision. Finally, a pair of multilayers was coated on silicon blanks in two steps, resulting in identical measured properties, with particular attention being given to the tangential direction of the elliptical shape. Figure 3 also shows that the non-linear accelerated movement of the mirrors can be improved further using better synchronized drives. The small deviations in theta or in multilayer thickness are most likely caused by imperfect drive synchronization. On this basis, it can be concluded that state-of-the-art multilayer fabrication is capable to fabricate consecutive mirrors with a deviation in thickness as small as $1\text{-}2$ pm.

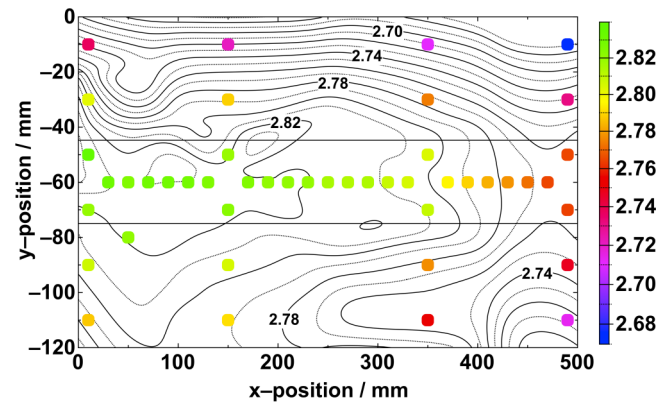


FIG. 4. Contour plot of the multilayer period of 200 Ru/C pairs over the whole optical area of 500 mm in length and 80 mm in width. The contour lines indicate 10 pm steps in height. They are smooth on the left- and nearly parallel on the right-hand side. In the tangential direction, the period decreases progressively from the left to the right-hand side due to the specified elliptical shape of the mirror.

D. Profile of the multilayer period on the picometer scale over the whole deposition area

All reflectometry measurements at the above-mentioned 46 mirror positions were analyzed using the Leptos R software package (Bruker Corporation) to obtain the X-ray optical properties, in particular, the Bragg angle and the multilayer period. The contour plot of the Ru/C multilayer period shown in Figure 4 demonstrates the variation of the period over the whole optical area of 500 mm in length and 80 mm in width. An elliptical shape in the tangential direction is clearly visible, since the period decreases progressively from the left to the right-hand side. The contour lines indicate 10 pm steps in height. On the right-hand side, the contour lines are nearly parallel, as would be expected with an ideal elliptically shaped cylinder. This result confirms the high precision of the d-spacing variation, which is achieved by using a mask during fabrication of a multilayer. Previous results of C and W single layers also showed a distinct improvement in the sagittal direction due to the use of an optimised mask, which has a width (waist) of about 71 mm in the center. Applying this enhancement, the percentage deviation in layer thickness for single layers is reduced to less than 2% .^{45,52} In the case of multilayers, the achievable range of the multilayer thickness gradient is restricted, since a previously coated thickness limits the change to a later deposited thickness due to the width of the mask. It is possible to achieve a higher dynamic in the thickness gradient by narrowing the width of the mask; however, this will increase the overall deposition time. This interplay between achievable thickness and mask size has to be optimized in a suitable way to fabricate the desired thickness profile along the mirror length.

E. Multilayer properties in the sagittal direction of the mirror

The sagittal variations in theta shown in Fig. 5 were measured at four x-positions ($x = 10, 150, 350, 490$ mm) indicated in Fig. 4. The four curves are nearly parallel but shifted with respect to each other due to the elliptical shape in

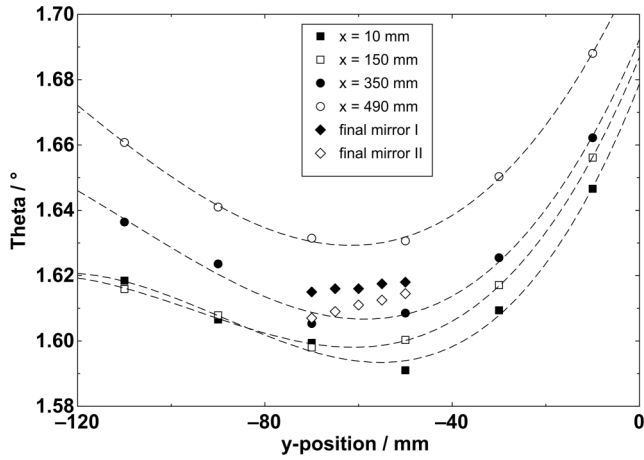


FIG. 5. Incidence angle as a function of the y -position (along the sagittal direction) of a multilayer mirror with 200 Ru/C pairs measured by Cu radiation. As expected the minimum is in the center at about $y = -60$ mm. The incidence angle increases to the outer area of the mirror, which was measured at 4 x -positions. The multilayer period is therefore reduced due to the limited area of uniform deposition. The four variations are nearly parallel but shifted with respect to each other due to the elliptical shape in theta in the tangential direction. The experimental results of two final mirrors with a small width of 30 mm are added. The first one is nearly constant. The second one was slightly angled during deposition, which causes a tilt in data.

thickness or in theta in the tangential direction. Each variation has its minimum at about $y = -60$ mm, which is at the center of the mirror, as expected. The experimental data of the center of the final two multilayer mirrors are included (open and full diamonds) and show that there is a slight shift between the left and the right-hand side of the mirror over a length of 20 mm. The difference in theta over this width of 20 mm is very small at a value of less than 0.008° ($140 \mu\text{rad}$). These experimental results illustrate that the multilayer fabrication is ultra-precise over the entire optical area. Moreover, it demonstrates that the unintended deviation in the precise mirror alignment between different runs is less than 0.2 mrad, which is most likely caused by a very small tilt of the mirror surface during its initial installation. The adjustment of the mirror surface is very important, in that the tangential and sagittal directions of the mirror are parallel to the x -direction (the moving direction of the carrier) and parallel to the y -direction, respectively. The exact alignment of a 30 mm small mirror is more difficult than the positioning of a 120 mm wide mirror. Therefore, allowing a slightly higher deviation in the sagittal direction of up to 0.36 mrad it becomes feasible to coat two mirrors side by side over a length of 60 mm. A one-step process would be time saving and very advantageous, since a single step would guarantee that the X-ray optical properties of both mirrors would be virtually identical, which is often a requirement for synchrotron applications.

F. Measured reflectivity of Ru/C multilayers

The reflectivity measurements were used to determine the local reflectivity and the FWHM of the first-order Bragg peak as a function of the number of Ru/C pairs at two photon energies (Fig. 6 and Table I). These X-ray optical properties are important when evaluating the performance of an X-ray

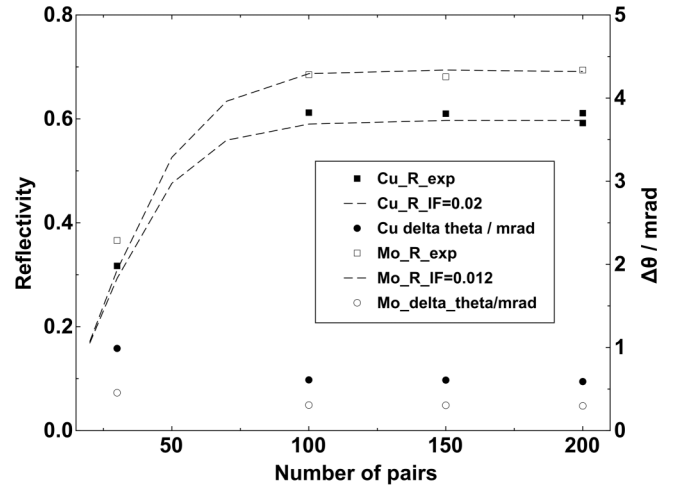


FIG. 6. Measured and simulated local reflectivity and FWHM of the first-order Bragg peak as a function of the number of Ru/C pairs measured at two photon energies.

mirror, in particular, its ability to transport the high flux of an X-ray beam with good spectral purity $\Delta\lambda/\lambda$. The overall performance of a multilayer mirror is always a function of the precision of the variation in multilayer period along the mirror length. It is therefore not necessary for the value of the d -spacing at a particular position to be accurate; however, it is important that the thickness gradient should be very precise over the mirror dimensions, that is, in the tangential and sagittal directions. The reflectivity scans were performed using Cu (8.048 keV) and Mo (17.48 keV) radiation to obtain experimental results above and below the relevant photon energy of 15 keV. In general, it is expected that the measured reflectivity should increase distinctly with increasing number of Ru/C pairs, while the FWHM should decrease slightly. Depending on the photon energy used the effective number of Ru/C pairs contributing to the reflectivity can be estimated using the equation¹

$$\frac{\Delta\lambda}{\lambda} = \frac{\Delta\theta}{\tan\theta} = \frac{1}{N_{\text{eff}}}. \quad (3)$$

The resulting number is approximately 100 pairs.

Due to convolution, the X-ray optical properties depend on the experimental conditions of the measurement. These are the dimensions and properties of X-ray source, slits, and detector and depend on the reflectometer. In the software package Leptos R, the measuring conditions can be taken into account using the resolution function, which depends on the

TABLE I. Measured (expt.) and calculated (cal.) reflectivity and measured Bragg peak width of Ru/C multilayers as a function of the number of pairs (for Cu and Mo radiation, calculated values are without geometrical factors).

Number of periods	$R_{\text{Cu}}/\%$ expt.	$R_{\text{Cu}}/\%$ cal.	$R_{\text{Mo}}/\%$ expt.	$R_{\text{Mo}}/\%$ cal.	$\Delta\theta_{\text{Cu}}/\text{mrad}$	$\Delta\theta_{\text{Mo}}/\text{mrad}$
30	32	33	32	36	0.99	0.46
100	59	72	71	89	0.61	0.31
150	61	74	71	92	0.60	0.30
200	60	74	73	92	0.59	0.30

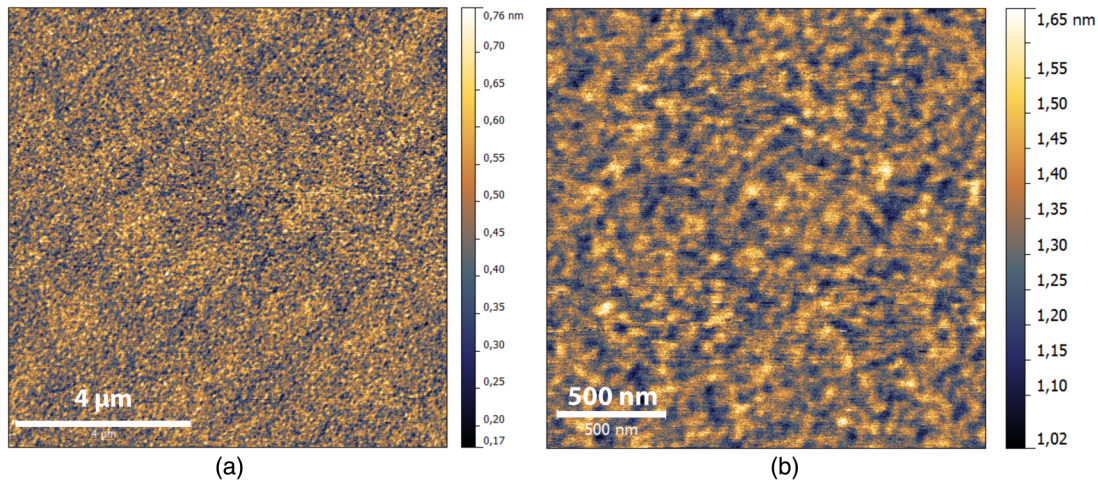


FIG. 7. AFM surface images from Ru/C multilayers measured over two areas of $10\ \mu\text{m} \times 10\ \mu\text{m}$ (left) and $2\ \mu\text{m} \times 2\ \mu\text{m}$ (right): The multilayers exhibit micro-roughness of 0.086–0.107 nm rms and 0.092–0.199 nm rms, respectively. The scale bars represent $4\ \mu\text{m}$ (left) and $500\ \mu\text{m}$ (right).

above-mentioned geometrical factors.⁵³ The values for the experimentally determined reflectivity and for the calculated reflectivity (without geometrical factors) for increasing numbers of periods (from 30 to 200 periods) are listed in Table I. A comparison between experimental results obtained using Cu and Mo radiation shows that an identical trend is clearly observed for both photon energies. In both cases the reflectivity increases distinctly and then saturates at a number of periods above 100 approximately 60% for Cu radiation and at approximately 70% for Mo radiation. Experimentally a reflectivity of about 60% has been measured for 150 Ru/C pairs using Cu radiation and a reflectivity of 70% has been measured for 200 Ru/C pairs using Mo radiation.

G. Surface quality of Ru/C multilayers

AFM measurements were performed of Ru/C multilayers deposited on a super-polished silicon substrate produced by Gooch & Housego. Two measuring areas are shown in Figs. 7(a) (left: $10\ \mu\text{m} \times 10\ \mu\text{m}$) and 7(b) (right: $2\ \mu\text{m} \times 2\ \mu\text{m}$). Before deposition, the substrate exhibited an initial roughness of less than 0.1 nm rms. After deposition of a multilayer with 200 pairs under optimum conditions, the surface roughness is nearly unchanged at about 0.1 nm rms on both measuring areas. This result confirmed the high quality of the multilayer process as well as its stability, reproducibility, and precision.

IV. CONCLUSIONS

The main tasks of multilayer fabrication are to find the best combination of layer materials and to accomplish a precise thickness variation along the mirror length. Both issues should achieve high photon reflectivity and high flux as required for the beamline applications. The challenge of this work is to accomplish a very tight elliptically shaped thickness variation of better than 0.3% with a period of 2.8 nm over a very long mirror length of 500 mm for future fabrication of a pair of mirrors with identical properties for a synchrotron

beamline with a photon energy of 15 keV. The results presented here show that the HZG magnetron sputtering facility is perfectly suited to fabricate single and multilayer mirrors within the required error margins. Magnetron sputtered Ru/C multilayers were investigated by means of transmission electron microscopy that allows us to assess the quality of the layer interface, thus enabling the sputtering conditions to be optimised. The HZG magnetron sputtering facility provides precise and flexible carrier movement with constant velocity, and both constant and non-uniform acceleration of the 1500 mm long carrier during the coating process. For X-ray mirror development, the fabrication of multilayers with constant and laterally graded d-spacings is now possible on the picometer scale along the entire deposition length. The X-ray reflectance measurements of Ru/C multilayers confirmed that the period varied from 2.825 nm at the left edge to 2.758 nm at the right edge in the tangential direction of a 500 mm long mirror. An error band of less than 0.2% was accomplished for the desired ideal elliptical cylinder. The contour plot of the periods measured over the entire area of 500 mm by 120 mm shows the elliptical reduction in the tangential direction and parallel lines in the sagittal direction. The experimental reflectivity of the calibration samples was determined to 60% and 72% using Cu (8.048 keV) and Mo (17.48 keV) radiation, which are above and below the specified photon energy of 15 keV for the synchrotron application. The experimental results confirm the ultra-high quality of the mirrors and state-of-the-art multilayer technology. In the near future, our ultra-precise thin-film fabrication will be employed to manufacture multiple stripes on one substrate for tomography applications. Such a mirror is able to switch between different photon energy ranges and provides a high flux in each range.

ACKNOWLEDGMENTS

We are grateful to the engineering department at HZG for their valuable support during the development, maintenance, and improvement of the new sputtering facility, especially to J. Buhrz for the sophisticated support to expand the possibilities of the software-controlled movement of the carrier, T.

Böttcher for the technical constructions to enhance stability and reproducibility of the facility, and G. Musielak for the fruitful maintenance to guarantee the mechanical reliability. We also thank the other employees at our technical department for their prompt support. Special thanks to all of my colleagues of the nanotechnology department.

- ¹D. Attwood, *Soft X-Rays and Extreme Ultraviolet Radiation* (Cambridge University Press, Cambridge, 1999), p. 69.
- ²E. Spiller, *Soft X-Ray Optics* (SPIE-The International Society for Optical Engineering, Bellingham, 1994), p. 139.
- ³B. L. Henke, E. M. Gullikson, and J. C. Davis, *At. Data Nucl. Data Tables* **54**, 181 (1993).
- ⁴Fachbereich Optische Technologien, X-ray optical systems—X-ray mirrors—Total reflection mirrors and multilayer mirrors, Technische Regel, Richtlinie ICS:17.180.30, VDI/VDE-Gesellschaft Mess- und Automatisierungstechnik, Düsseldorf, 2011.
- ⁵I. A. Makhotkin, E. Zoethout, E. Louis, A. M. Yakunin, S. Müllender, and F. Bijkerk, *Opt. Express* **20**, 11778 (2012).
- ⁶A. Rack, T. Weitkamp, M. Riotte, D. Grigoriev, T. Rack, L. Helfen, T. Baumbach, R. Dietsch, T. Holz, M. Krämer, F. Siewert, M. Meduna, P. Cloetens, and E. Ziegler, *J. Synchrotron Radiat.* **17**, 496 (2010).
- ⁷F. Siewert, J. Buchheim, S. Boutet, G. J. Williams, P. A. Montanez, J. Krzywinski, and R. Signorato, *Opt. Express* **20**, 4525 (2012).
- ⁸F. Siewert, J. Buchheim, T. Zeschke, M. Störmer, G. Falkenberg, and R. Sankari, *J. Synchrotron Radiat.* **21**, 968 (2014).
- ⁹J.-P. Guigay, Ch. Morawe, V. Mocella, and C. Ferrero, *Opt. Express* **16**, 12050 (2008).
- ¹⁰Ch. Morawe, J.-P. Guigay, V. Mocella, and C. Ferrero, *Opt. Express* **16**, 16138 (2008).
- ¹¹P. Ricardo, C. Novak, C. Michaelsen, J. Wiesmann, and R. Bormann, *Appl. Opt.* **40**, 2747 (2001).
- ¹²M. Schuster and H. Göbel, *J. Phys. D: Appl. Phys.* **28**, A270 (1995).
- ¹³M. Schuster, H. Göbel, L. Brügemann, D. Bahr, F. Burgäzy, C. Michaelsen, M. Störmer, P. Ricardo, R. Dietsch, T. Holz, and H. Mai, *Proc. SPIE* **3767**, 183 (1999).
- ¹⁴M. Bargheer, N. Zhavoronkov, R. Bruch, H. Legall, H. Stiel, M. Woerner, and T. Elsaesser, *Appl. Phys. B: Lasers Opt.* **80**, 715 (2005).
- ¹⁵M. Ohring, *Materials Science of Thin Films* (Academic Press, San Diego, 2002), p. 109.
- ¹⁶S. Swann, *Vacuum* **38**, 791 (1988).
- ¹⁷C. Liu, A. Macrander, J. Als-Nielsen, and K. Zhang, *J. Vac. Sci. Technol., A* **19**, 1421 (2001).
- ¹⁸E. N. Kotlikov, V. N. Prokashv, V. A. Ivanov, and A. N. Tropin, *J. Opt. Technol.* **76**, 100 (2009).
- ¹⁹T. Fujimoto, B. Li, I. Kojima, S. Yokoyama, and S. Murakami, *Rev. Sci. Instrum.* **70**, 4362 (1999).
- ²⁰C. Montcalm, R. F. Grabner, R. M. Hudyma, M. A. Schmidt, E. Spiller, C. C. Walton, M. Wedowski, and J. A. Folta, *Appl. Opt.* **41**, 3262 (2002).
- ²¹E. Louis, E. D. van Hattum, S. Alonso van der Westen, P. Sallé, K. T. Grootkarzijn, E. Zoethout, and F. Bijkerk, *Proc. SPIE* **7636**, 76362T (2010).
- ²²E. Louis, E. Zoethout, R. W. E. van de Kruijs, I. Nedulcu, A. E. Yakshin, S. Alonso van der Westen, T. Tsarfati, and F. Bijkerk, *Proc. SPIE* **5751**, 1170 (2005).
- ²³E. Louis, A. E. Yakshin, T. Tsarfati, and F. Bijkerk, *Prog. Surf. Sci.* **86**, 255 (2011).
- ²⁴Y. S. Chu, C. Liu, D. C. Mancini, F. De Carlo, A. T. Macrander, B. Lai, and D. Shu, *Rev. Sci. Instrum.* **73**, 1485 (2002).
- ²⁵A. Haibel, F. Beckmann, T. Dose, J. Herzen, M. Ogurreck, M. Müller, and A. Schreyer, *Powder Diff.* **25**, 161 (2010).
- ²⁶A. Rack, T. Weitkamp, I. Zanette, Ch. Morawe, A. Vivo Rommeveaux, P. Tafforeau, P. Cloetens, E. Ziegler, T. Rack, A. Cecilia, P. Vagovic, E. Harmann, R. Dietsch, and H. Rieseemeier, *Nucl. Instrum. Methods Phys. Res., Sect. A* **649**, 123 (2011).
- ²⁷A. Rack, T. Weitkamp, L. Assoufid, T. Rack, I. Zanette, Ch. Morawe, R. Kluender, and C. David, *Nucl. Instrum. Methods Phys. Res., Sect. A* **710**, 101 (2013).
- ²⁸T. Bigault, E. Ziegler, C. Morawe, R. Hustache, J.-Y. Massonnat, and G. Rostaing, *Proc. SPIE* **5195**, 12 (2003).
- ²⁹K. J. S. Sawhney, I. P. Dolbnya, S. M. Scott, M. K. Tiwari, G. M. Preece, S. G. Alcock, and A. W. Malandain, *Proc. SPIE* **8139**, 813908 (2011).
- ³⁰P. Kirkpatrick and A. V. Baez, *J. Opt. Soc. Am.* **38**, 766 (1948).
- ³¹C. Morawe and M. Osterhoff, *Nucl. Instrum. Methods Phys. Res., Sect. A* **616**, 98 (2010).
- ³²M. Stampanoni, F. Marone, G. Mikuljan, K. Jefimovs, P. Trtik, J. Vila-Comamala, C. David, and R. Abela, *Proc. SPIE* **7078**, 70780V (2008).
- ³³K. Ichyanagi, T. Sato, S. Nozawa, K. H. Kim, J. H. Lee, J. Choi, A. Tomita, H. Ichikawa, S. Adachi, H. Ihee, and S. Koshihara, *J. Synchrotron Radiat.* **16**, 391 (2009).
- ³⁴H. Jiang, Y. He, Y. He, A. Li, H. Wang, Y. Zheng, and Z. Dong, *J. Synchrotron Radiat.* **22**, 1379 (2015).
- ³⁵T. D. Ngyuen, R. Gronsky, and J. B. Kortright, *Mater. Res. Soc. Symp. Proc.* **230**, 109 (1992).
- ³⁶C. C. Walton and J. B. Kortright, *Mater. Res. Soc. Symp. Proc.* **382**, 369 (1995).
- ³⁷S. Bajt, *J. Vac. Sci. Technol., A* **18**, 557 (2000).
- ³⁸I. V. Kozhevnikov, E. O. Filatova, A. A. Sokolov, A. S. Konashuk, F. Siewert, M. Störmer, J. Gaudin, B. Keitel, L. Samoylova, and H. Sinn, *J. Synchrotron Radiat.* **22**, 348 (2015).
- ³⁹M. Störmer, F. Siewert, and H. Sinn, *J. Synchrotron Radiat.* **23**, 50 (2016).
- ⁴⁰J. Chalupsky, V. Hajkova, V. Altapova, T. Burian, A. J. Gleeson, L. Juha, M. Jurek, H. Sinn, M. Störmer, R. Sobierajski, K. Tiedtke, S. Toleikis, T. Tschentscher, L. Vysin, H. Wabnitz, and J. Gaudin, *Appl. Phys. Lett.* **95**, 031111 (2009).
- ⁴¹H. Sinn, J. Gaudin, L. Samoylova, A. Trapp, and G. Galasso, “Conceptual design report: X-ray optics and beam transport,” Technical Note, XFEL.EU TN-11-002 (European XFEL GmbH, Hamburg, Germany, 2011).
- ⁴²A. Aquila, R. Sobierajski, C. Ozkan, V. Hájková, T. Burian, J. Chalupský, L. Juha, M. Störmer, S. Bajt, M. T. Klepka, P. Dłuzewski, K. Morawiec, H. Ohashi, T. Koyama, K. Tono, Y. Inubushi, M. Yabashi, H. Sinn, T. Tschentscher, A. P. Mancuso, and J. Gaudin, *Appl. Phys. Lett.* **106**, 241905 (2015).
- ⁴³I. V. Kozhevnikov, A. V. Buzmakov, F. Siewert, K. Tiedtke, M. Störmer, L. Samoylova, and H. Sinn, *J. Synchrotron Radiat.* **23**, 78 (2016).
- ⁴⁴M. Störmer, C. Horstmann, D. Häussler, E. Speiker, F. Siewert, F. Scholze, F. Hertlein, W. Jäger, and R. Bormann, *Proc. SPIE* **7077**, 707705 (2008).
- ⁴⁵M. Störmer, C. Horstmann, F. Siewert, F. Scholze, M. Krümmey, F. Hertlein, M. Matiaske, J. Wiesmann, and J. Gaudin, *AIP Conf. Proc.* **1234**, 456 (2010).
- ⁴⁶D. L. Windt, *Comput. Phys.* **12**, 360 (1998).
- ⁴⁷A. Ulyanenko and S. Sobolewski, *J. Phys. D: Appl. Phys.* **38**, 235 (2005).
- ⁴⁸G. Binnig, C. F. Quate, and C. Gerber, *Phys. Rev. Lett.* **56**, 930 (1986).
- ⁴⁹E. Meyer, *Prog. Surf. Sci.* **41**, 3 (1992).
- ⁵⁰T. B. Massalski, *Binary Alloy Phase Diagrams* (ASM International, Materials Park, OH, 1990).
- ⁵¹U. Bonse, G. Materlik, and W. Schröder, *J. Appl. Crystallogr.* **9**, 223 (1976).
- ⁵²M. Störmer, F. Siewert, and J. Gaudin, *Proc. SPIE* **8078**, 80780G (2011).
- ⁵³A. Gibaud, G. Vignaud, and S. K. Sinha, *Acta Crystallogr., Sect. A: Found. Crystallogr.* **49**, 642 (1993).